Am J Transl Res 2021;13(3):1535-1547
www.ajtr.org /ISSN:1943-8141/AJTR0119517

Original Article

Role of kynurenine in promoting the generation of exhausted CD8$^+$ T cells in colorectal cancer

Dandan Wu[1], Yufeng Zhu[2]

[1]*Department of Gastroenterology, The First Affiliated Hospital of Jinzhou Medical University, Jinzhou 121000, China;* [2]*Department of General Surgery, The First Affiliated Hospital of Jinzhou Medical University, Jinzhou 121000, China*

Received August 4, 2020; Accepted January 11, 2021; Epub March 15, 2021; Published March 30, 2021

Abstract: Although blocking programmed cell death protein 1 (PD-1) has emerged as a standard treatment for metastatic colorectal cancer (CRC), a vast majority of CRC patients still respond poorly to anti-PD-1 immunotherapy. In this study, we showed that the levels of indoleamine 2,3-dioxygenase 1 (IDO1) and its catabolite kynurenine (Kyn) were higher in late stages (stages III and IV) than in early stages (stages I and II) of CRC patients. We found that Kyn could induce the expression of immune checkpoints and exhaustion markers in CD8$^+$ tumor-infiltrating T cells. Knockdown of IDO1 expression using small hairpin RNAs (shRNAs) in the MC38 and CT26 colorectal cell lines led downregulation of Kyn expression and activation of CD8$^+$ T cells in MC38- or CT26-bearing mice. Subsequent mechanistic study revealed significantly reduced thymocyte selection-associated HMG box (TOX) mRNA levels in CD8$^+$ tumor-infiltrating T cells isolated from IDO1 knockdown MC38-Scr- and CT26-bearing mice. Kyn-induced CD8$^+$ T cell exhaustion was reversed by knockdown of TOX expression. Finally, the application of the well-known IDO1 inhibitors 1MT or NLG919 substantially improved the therapeutic effect of CRC *in vivo* and restored CD8$^+$ tumor-infiltrating T cells anti-tumor activity. This improvement was further enhanced by an anti-PD-1 combined therapy. In conclusion, our study revealed a novel mechanism underlying the metabolic factors found in tumor microenvironment which could induce CD8$^+$ T cells exhaustion. Our findings provided a new strategy of restoring the antitumor activity of CD8$^+$ T cells through combined targeting of the IDO1/Kyn and PD-1/PD-L1 pathways in patients with CRC.

Keywords: Indoleamine 2,3-dioxygenase 1, kynurenine, colorectal cancer, CD8$^+$ T, exhaustion

Introduction

Impaired antitumor functions of cytotoxic T lymphocytes result in uncontrolled tumor growth in multiple cancer types. One reason for this is the induction of CD8$^+$ tumor-infiltrating T cells exhaustion by the immunosuppressive tumor microenvironment [1-4]. Exhausted CD8$^+$ T cells are characterized by high expression levels of exhaustion markers such as programmed cell death protein 1 (PD-1), cytotoxic T-lymphocyte-associated protein 4 (CTLA-4), and lymphocyte-activation gene 3 (LAG3) as well as impaired cytokine IFN-γ and TNF-α production [5, 6]. Currently, immune checkpoint inhibitors (ICIs) such as anti-PD-1 or anti-CTLA-4 antibody therapy have been developed to abrogate the CD8$^+$ T-cell exhaustion status and improve the prognosis of various cancer types in the clinical setting [7-15].

Colorectal cancer (CRC) is the major cause of cancer death worldwide and is categorized into the mismatch repair-deficient and microsatellite instability-high (dMMR-MSI-H) signature with a high overall mutation burden (>12 mutations per 10^6 DNA bases) and mismatch repair-proficient and microsatellite instability-low signature with a much lower mutation burden (<8.24 mutations per 10^6 DNA bases) [16-18]. In dMMR-MSI-H CRC, PD-1 inhibition is associated with strong clinical benefits with objective response and disease control rates of 60% and 84%, respectively [19-21]. However, the vast majority of patients with dMMR-MSI-H CRC don't not respond to immunotherapy previously [22]. The suppressive tumor microenvironment has a unique metabolic restriction involving the development and maintenance of T cell exhaustion status. Therefore, understanding the metabolic factors in tumor microenvironment would

help develop new strategies to target immune checkpoints.

Tryptophan catabolism has recently been recognized as an important tumor microenvironment factor in suppressing T cell-mediated antitumor immune responses [23-27]. Tryptophan catabolites, particularly kynurenine (Kyn), inhibits T cell-mediated immune responses in various types of disease [28, 29]. A recent study reported that tumor cells derived Kyn induced PD-1 upregulation in $CD8^+$ T cells [30]. Therefore, we hypothesize that Kyn plays an important role in inducing $CD8^+$ T-cell exhaustion in CRC.

In the present study, we examined the potential mechanisms underlying the effect of Kyn in the tumor microenvironment of CRC patients. We found that tumor cell-derived Kyn induced the generation of $CD8^+$ T cells exhaustion phenotype by upregulating TOX expression in CRC. Our findings would provide a new strategy of combined PD-1 blockade and Kyn production for the clinical treatment of CRC.

Materials and methods

Cells and reagents

CT26, Mc38 and Mc38-OVA cell line were purchased from ATCC (CRL-2638, USA), *China Center for Type Culture Collection* (3111C000-1CCC000523, China) and Biovector (ntcc69-0052, China), respectively. These cell lines were all preserved in DMEM (10829018; Thermo Fisher Scientific, CA Canoga Park), containing 10% fetal bovine serum (Gibco, Australia), 1% glutamine (Thermo Fisher Scientific, USA), 1% MEM nonessential amino acids (Gibco, USA), 100 μg/ml and streptomycin 100 U/ml penicillin (Solarbio, China). All cells were grown in a monolayer at 37°C and 5% CO_2 under standard conditions. These cells were identified by short tandem repeat (STR) typing. Mycoplasma in cells was detected by PCR.

Patients and ethics

Twenty cases of colon cancer tissues were collected from The First Affiliated Hospital of Jinzhou Medical University. After surgical resection, they were directly preserved with liquid nitrogen. All patients were given a written informed consent form and the research was approved by Ethics committee of the First Affiliated Hospital of Jinzhou Medical University (No. 202030). We use the seventh edition of the American Joint Committee on Cancer staging system (AJCC-7) for colon cancer pathological staging. All the included patients did not receive any radiotherapy or chemotherapy before operation.

ELISA for Kyn and correlation analysis

Kynurenine (KYN) from tumor tissue and serum was quantified using Kynurenine (KYN) ELISA Kit (E4629, BioVision, USA) following the manufacturer's protocol. The correlations between kynurenine content and the percentages of checkpoint markers were statistically evaluated using Pearson correlation (PC) tests. The statistics package, SPSS for Windows (version 23.0, SPSS Inc., Chicago, IL, USA) was used for determining the significance based on the validated *p*-value of 0.05.

Mice

6-weeks-old female CD45.1 C57BL/6J mice were purchased from Shanghai Model Organisms Center. 6-week-old female CD45.2 C57BL/6J and BALB/C mice were purchased from Beijing Vital River Laboratory Animal. OT-I transgenic mice were purchased from Jackson Laboratory. All the murine experiments were conducted following the guidelines of animal care and use of the Committee of the First Affiliated Hospital of Jinzhou Medical University. This study was specially approved by the experimental animal welfare and ethics committee of the First Affiliated Hospital of Jinzhou Medical University (No. 202030).

Murine T cells purification and adoptive transfer

We obtained single splenocyte suspension by crushing spleen grinding fluid with 40 μm nylon cell filter (FALCON, USA). $CD8^+$ T cell were purified using mouse $CD8^+$ T cell enrichment Kit (Miltenyi Biotec, Germany) following the manufacturer's protocol. 5×10^5 naïve OT-1 CD45.1 $CD8^+$ T cells (or siTOX transduction) were transferred into the MC38-ova tumor bearing mice every 3 day for 3 times.

Cell transfection

To knockdown IDO expression, we purchased Retroviral IDO-shRNA (Hanbio, China). MC38

cells and CT26 cells in logarithmic phase were inoculated into a 24-well plate with a cell density of 1 × 10^5/well. When cells reached about 60% fusion, retroviruses coating with 8 μg/ml Polybrene (Sigma Aldrich, Germany) were transfected into these cells. Cells were harvested for analyzing the IDO knockdown efficiency after 48 hours. To knockdown Tox expression in $CD8^+$ T cells, TOX siRNA was purchased (Ribobio China) and transformed into pre-activated naive $CD8^+$ T cells by Lonza amaxa 4D. 48 hours after transfection, cells were harvested for analyzing TOX knockdown efficiency. High efficiency knockdown siRNA was selected for the subsequent experiments.

Tumor model in vivo

5 × 10^5 MC38 (NC or ShIDO-transduced) or CT26 (NC or ShIDO-transduced) cells were implanted subcutaneously into 8-10-week-old female C57BL/6J and BALB/C mice. The tumor size was measured by electronic caliper every 5 days. The tumor volume was calculated as shortest diameter^2 × longest diameter/2. Once the tumor exceeds 20 mm in any dimension, euthanasia is performed.

Mice were randomly divided into different treatment group 5 days after cells injection. 50 μg 1-MT, 50 μg NLG919, 50 μg 1-MT + 100 μg PD-1 antibody or 50 μg NLG919+100 μg PD-1 antibody were intraperitoneally injected every two days for 5 times.

For adoptive transfer, 5 × 10^5 OT-I CD45.1 $CD8^+$ T cells (or siTOX transduction) were transferred into the MC38-OVA tumor bearing mice 5 days after 1 × 10^6 MC38 OVA cells injection.

Isolation of tumor infiltrating lymphocytes (TIL)

A single cell suspension was prepared from the tumor of MC38-bearing mice by mechanical separation, then TILs were isolated from single cell suspensions using Mouse Tumor Dissociation Kit (Miltenyi, Germany) according to the manufacturer's protocol. The TILs were either for subsequent flow cytometry analysis or sorting.

Flow cytometry and antibody

$CD8^+$ T cells of tumor infiltrating lymphocytes were purified by flow cytometry-assisted cell sorting. The purity of sorted cells was more than 95%. To detect cytokine production, lymphocytes were stimulated for 2 hours in the presence of cell stimulating mixture (Ebioscience, USA), then stained with surface markers anti-LAG-3 (Biolegend, USA), anti-PD-1 (Biolegend, USA) and CTLA4 (Biolegend, USA) with 1:100 dilute in PBS with 1% FBS. After incubating on ice for 30 min, Cell Fixation/Permeation Kit (BD, USA) and Transcription Factor Fixation/Permeabilization Buffer (Biolegend, USA) were used for intracellular cytokine and nuclear transcriptional factors staining respectively. Cells were fixed for 30 min followed by washing with Permeabilization Buffer twice, then stained with anti IFN-γ (Biolegend, USA), anti-TNFα (Biolegend, USA) and anti-TOX (Miltenyi Biotec, Germany) with 1:50 dilute in Permeabilization Buffer in 4°C overnight. Flow cytometry data were obtained by BD FACSCelesta (BD, USA) and analyzed by Flowjo software. The antibodies and reagents used for flow cytometry staining are listed in Table S2. All analyses were performed by t test using Graphpad Prism 8. P<0.05 (two-tailed) was considered statistically significant.

Quantitative RT-PCR

Different concentration gradients of kyn were applied for CD8 T cells stimulation. After 24 or 48 hours, cells were lysed in TriQuick Reagent (R1100, Solarbio, China). Total RNA was extracted according to the manufacture's protocol and stored in -80°C for future experiments. Reverse-transcription assay was carried out to obtain cDNA with a Universal RT-PCR Kit (M-MLV, free Taq polymerase) (RP1105, Solarbio, China).

Primer sequences: TOX: GCTCCCGTTCCATCCACAAA-3' (sense); 5'-TCCCAATCTCTTGCATCACAGA-3' (antisense). β-actin: GGCTGTATTCCCCTCCATCG-3' (sense); 5'-CCAGTTGGTAACAATGCCATGT-3' (antisense).

To quantify TOX expression, we use the qRT-PCR method to determine the mRNA levels and normalize it to β-actin. Toolkits are as follows: 2 × SYBR Green PCR Mastermix (SR1110, Solarbio, China) and CFX96 Touch Real-Time System (Bio-Rad).

Western blot

Total protein was extract from frozen tumor samples using a RIPA buffer (high) (R0010, Solarbio, China) containing protease Inhibitor Cocktail Set VI (539133, Solarbio, China) on ice for 30 min, then centrifuged at 14000 g for 15 min to get supernatant. Protein concentrations were determined by BCA assay (P0009, Beyotime, China). Protein samples (50 μg) were boiled with SDS-PAGE Sample Loading Buffer (P0015L, Beyotime, China) to linearized peptide chain, loaded and separated by SDS-PAGE on 8-12% tris-glycine gels before being transferred onto nitrocellulose membranes. The membrane was incubated with primary antibodies diluted with 5% skim-milk as followings: anti-mouse IDO1 (1:1,000 dilution, Cell Signaling Technology), anti-mouse GAPDH (1:5000 dilution, Cell Signaling Technology) at 4°C, overnight. Secondary horseradish peroxidase-coupled antibodies (A0208, Beyotime, China) was then used at 1:3000 for conjugating with primary antibody. Visualization by enhanced chemiluminescence was carried out according to the manufacturer's protocol (BeyoECL Moon, P0018FS, Beyotime, China).

Chromatin immunoprecipitation PCR

Samples were fixed with 1% formaldehyde at room temperature for 10 min to cross-link proteins and DNA, then neutralized with glycine (125 mM) for 5 min. Chromatin immunoprecipitation was performed by ChIP Assay Kit (P2078, Beyotime, China). Cells were lysed to liberate cellular components. Chromatin was fragmented to about 500 bp long by ultrasound. Target regions were pulled down by relevant antibodies and sorted out by magnetic beads. Purified DNA was then obtained by reversal crosslinking. The obtained DNA was subjected to quantitative PCR for PD-1, CTLA4, LAG3 promoter detection.

PD1: 5'-TCTGAACCTACAGGGGTGTC-3' (sense); 5'-CCTGGCTTTGGTACCTATGG-3' (antisense). CTLA4: 5'-TCAGACATCAGCTCCAGGAC-3' (sense); 5'-ACAAGCAAATCCATGGATGG-3' (antisense). LAG3: 5'-AATGCCTGTGAGCCTCAA-3' (sense); 5'-CTGCCTAGCCTTTCAGCATC-3' (antisense).

Dual luciferase reporter assay

Dual luciferase reporter assay was performed using Dual-Lumi™ II Luciferase Reporter Gene Assay Kit (RG089S, Beyotime, China) in a Modulus II Microplate Multimode Reader (Turner Biosystems). 48 hours after transfection, cells were lysed and collected. Briefly, dual-Glo luciferase substrate was added to each well in a 96-well plate and incubated at room temperature for 10 minutes. The firefly luminescence signal was recorded by multimode reader. A second Stop-Glo substrate was incubated for another 10 minutes. The Renilla luciferase signal was recorded. Data was calculated and normalized to control wells.

Statistical analysis

All murine experiments were randomly allocated and grouped before treatment. Sample sizes were at five to ten animals per experiment to ensure adequate statistical power. Statistical significance was calculated by paired two-sided t-tests and by one-way analysis of variance (ANOVA) with post-hoc Tukey's test for more than two groups in Graphpad Prism 8. The relationship Analysis was analyzed using SPSS for Windows (version 23.0, SPSS Inc., Chicago, IL, USA).

Results

Tumor cell-derived Kyn induced the generation of the exhausted CD8+ T-cell phenotype

To determine whether tumor cell-derived Kyn is responsible for the development and maintenance of the exhaustion phenotype of CD8+ T cells, Kyn content in colon tissues from CRC patients of different stages was measured by ELISA. Kyn content was found to be significantly elevated in late stages (stages III and IV) than in early stages (stages I and II) in both colon tissue and plasma from patients with CRC (**Figure 1A** and **1B**; Table S1). Further correlation studies showed that plasma Kyn content was positively correlated with PD-1, CTLA-4, and LAG3 expressions on CD8+ T cells (**Figure 1C**). CD8+ T cells were freshly isolated from the peripheral blood of healthy controls and cultured with different Kyn concentrations. PD-1, CTLA-4, and LAG3 (Antibody information in Table S2) expressions on CD8+ T cells were found to be significantly promoted by Kyn treatment in a concentration-dependent manner (**Figure 1D** and **1E**). Cytokine IFN-γ and TNF-α production by CD8+ T cells was inhibited by *in vitro* Kyn treatment in a dose-dependent manner (**Figure 1F** and **1G**). Taken together, these results suggested that

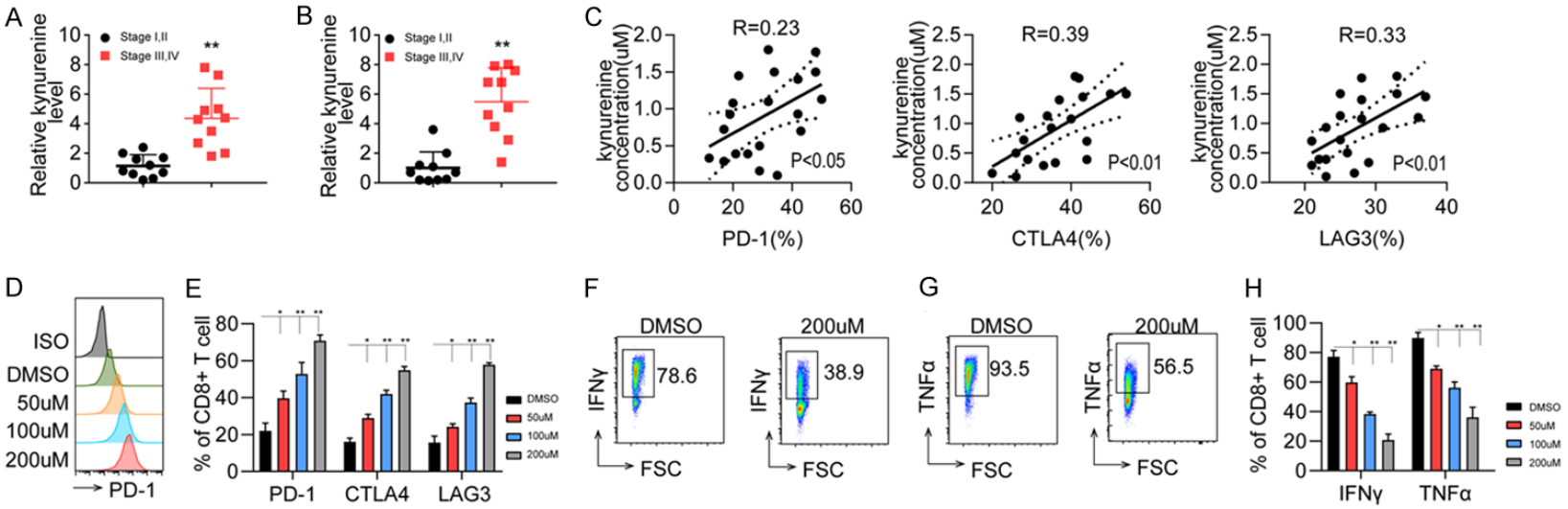

Figure 1. Kynurenine (Kyn)-induced CD8+ T-cell exhaustion. Kyn levels in (A) tissues and (B) plasma from patients with colorectal cancer (CRC) determined by ELISA (n = 10/group). Patient information in Table S1. (C) The percentages of PD-1, CTLA-4, and LAG3 expression on peripheral CD8+ T cells were measured by flow cytometry and correlated with Kyn levels in patients with CRC (n = 20). (D) Peripheral CD8+ T cells isolated from patients with CRC treated with 50, 100, and 200 μM Kyn. Representative flow cytometry histogram of PD-1 in CD8+ T cells was displayed. (E) PD-1, CTLA-4, and LAG3 expressions and (F-H) TNFα and IFN-γ production in CD8+ T cells were detected by flow cytometry. *P < 0.05, **P < 0.01, n.s no significant difference, (A and B) were analyzed by Student's t test, (C) was analyzed by Pearson's correlation test, (E and H) were analyzed by 1-way ANOVA. The data represent mean ± SEM (A-C, E and H).

tumor cell-derived Kyn promotes CD8+ T-cell exhaustion, resulting in the lack of anti-tumor immunity in CRC.

Enhanced indoleamine 2,3-dioxygenase 1 (IDO1) enzyme activity promoted CD8+ T-cell exhaustion in CRC

IDO1 catalyzes the commitment step of the Kyn metabolic pathway. These results prompted us to determine whether IDO1/Kyn pathway is involved in the promotion of the exhausted CD8+ T-cell phenotype. Interestingly, IDO1 expression was found to be higher in late stages (stages III and IV) than in early stages (stages I and II) in tissues from patients with CRC (**Figure 2A** and **2B**). We further knocked down IDO1 expression in MC38 and CT26 cell lines using small hairpin RNAs (shRNAs) and the knockdown efficiency was determined by western blot (**Figure 2C**). Inhibition of IDO1 activity led to the decreased concentration of Kyn in tissues from MC38- and CT26-bearing mice (**Figure 2D** and **2E**). Exhaustion-associated surface markers, PD-1, CTLA, and LAG3, were remarkably downregulated on tumor-infiltrating CD8+ T cell from the MC38-Scr-, MC38-IDO1-ShRNA#1-, and MC38-IDO1-ShRNA#2-bearing mice (**Figure 2F**). Furthermore, cytokines IFN-γ and TNF-α secretion were impaired by tumor-infiltrating CD8+ T cells (**Figure 2G-I**). Consistently, the same phenomenon was also observed on CT26 mouse model (**Figure 2J**, **2K**).

IDO1/Kyn promoted CD8+ T-cell exhaustion by up-regulating TOX expression in CRC

Next, we explored whether enhanced IDO1/Kyn activity promotes CD8+ T-cell exhaustion by regulating the activity of TOX, which is a key inducer of the canonical features of T-cell exhaustion. IDO1 knockdown in MC38 or CT26 could significantly reduce TOX mRNA levels in CD8+ T cell isolated from MC38-Scr- and CT26-bearing mouse (**Figure 3A**, **3B**). Consistently, TOX expression was also remarkably downregulated on the surface of CD8+ T cell isolated from IDO1 shRNA-treated tumor tissues than the negative control tissues (**Figure 3C** and **3D**). Freshly isolated mouse CD8+ T cells were treated with different concentrations of Kyn, and TOX mRNA level in CD8+ T cells was significantly upregulated in a concentration-dependent manner (**Figure 3E**). Kyn continuously induce increased TOX expression in CD8+ T cells depending on the concentration and time (**Figure 3F**). To further elucidate the relationship between Kyn and TOX in CD8+ T-cell exhaustion in CRC, TOX expression was knocked down by siRNA and its efficiency was confirmed by flow cytometry (**Figure 3G**). PD-1, CTLA-4, and LAG3 expressions were upregulated and cytokine IFN-γ and TNF-α production were down-regulated in CD8+ T cells treated with Kyn than DMSO in vitro, but reversed after the knockdown of TOX expression. These indicate that TOX is an important regulator of Kyn-induced CD8+ T-cell exhaustion in patients with CRC (**Figure 3H**).

To determine whether TOX binds to Pdcd1, Ctla-4, and Lag3 gene promoters in response to Kyn treatment, chromatin immunoprecipitation assay was performed. Kyn-treated CD8+ T cells increased the TOX binding activity of *Pdcd1*, *Ctla-4*, and *Lag3* gene promoters compared with control CD8+ T cells (**Figure 3J**). Furthermore, dual-luciferase reporter assay showed that TOX-over-expressed NIH3T3 cells increased PD-1, CTLA-4, and LAG3 promoter activity (**Figure 3K**). Next, we tested whether knocking down TOX can reverse the exhaustion status of tumor infiltrating CD8+ T cells from CRC murine model. As we expect, after transferring CD45.1+OT-1 T cells in tumor-bearing mice, TOX-silenced tumor infiltrating CD45.1+CD8+ T cells from tumor tissue expressed reduced levels of inhibitory receptors and demonstrated enhanced cytokine production (**Figure 3L**, **3M**).

Blocking IDO1 activity improved the therapeutic outcome of CRC by reversing the CD8+ T-cell exhaustion status

Finally, to examine whether manipulation of IDO1 activity in CRC cells affects tumor growth and CD8+ T cell-mediated antitumor immune responses, MC38-Scr, MC38-IDO1-sh1, and MC38-IDO1-sh2 cells were inoculated. Tumor growth and survival rate were measured at various time points after injection. MC38-IDO1-sh-bearing mice showed a more significant tumor regression and higher survival rate than MC38-scr-bearing mice (**Figure 4A**, **4B**). Similar phenomenon was observed in CT26-IDO1-sh-bearing mice (**Figure 4C**, **4D**). The tumor size was significantly smaller in CT26-IDO1-sh-bearing mice compared with control littermates

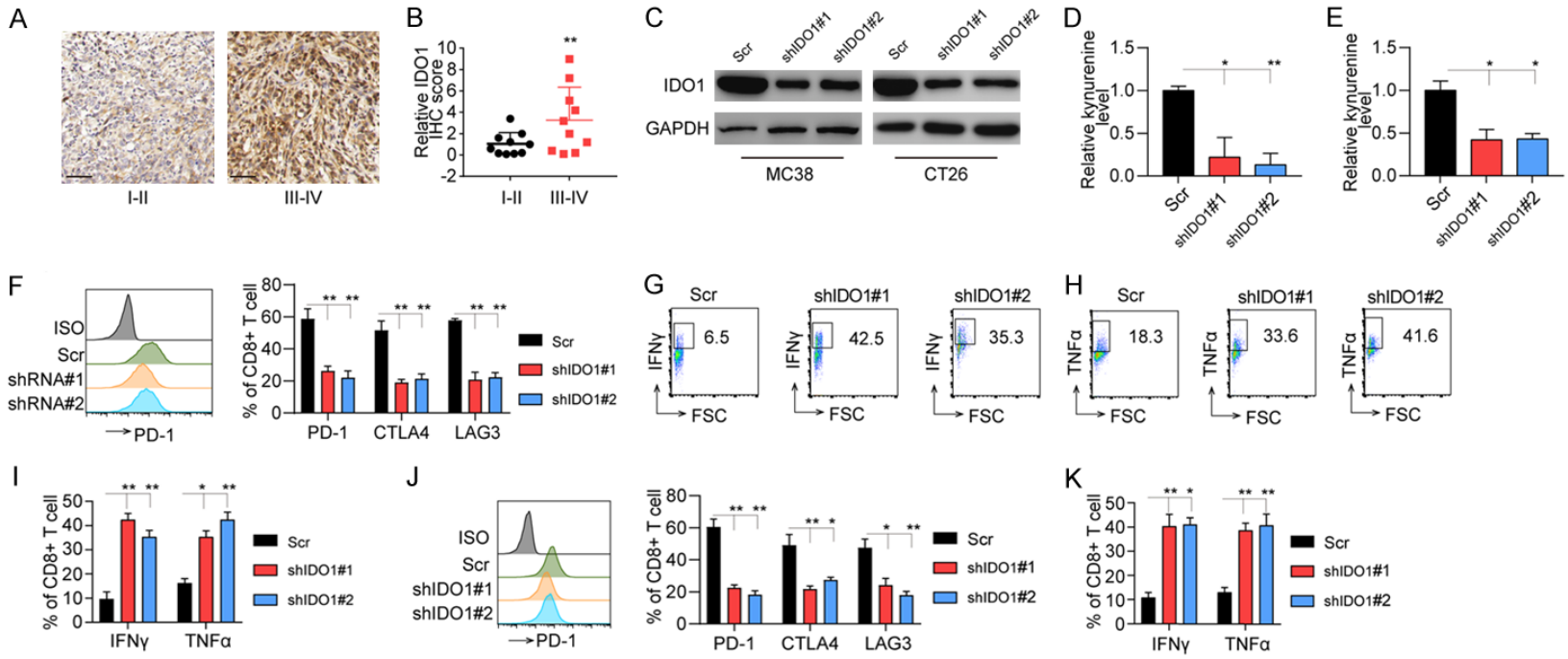

Figure 2. Blocking IDO1 activity in colorectal cancer (CRC) tumor cells reversed the CD8⁺ T-cell exhaustion phenotype. (A, B) IDO1 expression was analyzed by immunohistochemical staining of tissues from patients with CRC (n = 20). Scale bar: 50 μm. (C) Western blot analysis of IDO1 level in MC38-Scr, MC38-IDO1-ShRNA#1, MC38-IDO1-ShRNA#2, CT26-Scr, CT26-IDO1-ShRNA#1, and CT26-IDO1-ShRNA#2 cells treated with IFNγ (50 ng/ml) for 48 h. (D) Kynurenine (Kyn) levels in MC38-Scr, MC38-IDO1-ShRNA#1, and MC38-IDO1-ShRNA#2 tissues were determined using ELISA (n = 6). (E) Kyn levels in CT26-Scr, CT26-IDO1-ShRNA#1, and CT26-IDO1-ShRNA#2 tissues were determined by ELISA (n = 6). (F-H) Exhaustion marker expressions and cytokine production in CD8⁺ tumor-infiltrating lymphocytes isolated from MC38-Scr-, MC38-IDO1-ShRNA#1-, and MC38-IDO1-ShRNA#2-bearing mouse were measured using flow cytometry (n = 6). (J, K) Exhaustion marker expressions and cytokine production in CD8⁺ tumor-infiltrating lymphocytes isolated from CT26-Scr-, CT26-IDO1-ShRNA#1-, and CT26-IDO1-ShRNA#2-bearing mouse were measured using flow cytometry (n = 6). The scale bar is 50 μm. *P < 0.05, **P < 0.01, n.s no significant difference. B was analyzed by Student's t test. (D-F, I-K) were analyzed by 1-way ANOVA. The data represent mean ± SEM (B, D-F, I-K).

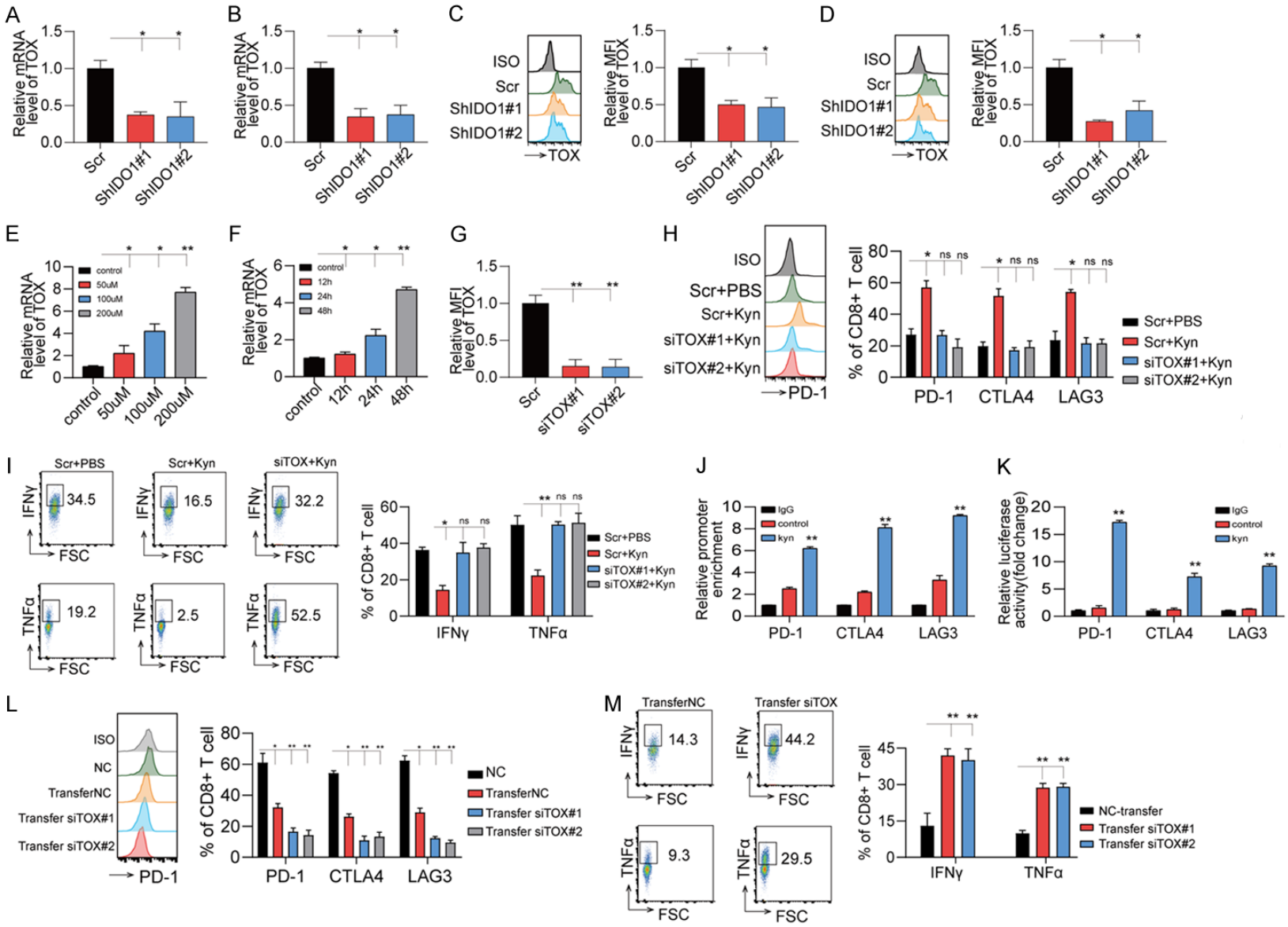

Figure 3. IDO1/Kynurenine (Kyn)-induced CD8⁺ T-cell exhaustion by regulation of TOX activity. (A) qRT-PCR analysis of TOX mRNA level in CD8⁺ tumor-infiltrating lymphocytes (TILs) isolated from MC38-Scr cells, MC38-IDO1-ShRNA#1 tissue, and MC38-ShRNA#2 tissues (n = 6/group). (B) qRT-PCR analysis of TOX mRNA level

in CD8+ TILs isolated from CT26-Scr cells, CT26-IDO1-ShRNA#1 tissue, and CT26-ShRNA#2 tissues (n = 6). (C) Flow cytometry analysis of TOX expression in CD8+ TILs isolated from MC38-Scr-, MC38-IDO1-ShRNA#1-, and MC38-IDO1-ShRNA#2-bearing mice (n = 6/group). (D) Flow cytometry analysis of TOX expression in CD8+ TIL of CT26-Scr-, CT26-IDO1-ShRNA#1-, and CT26-IDO1-ShRNA#2-bearing mice (n = 6/group). (E) qRT-PCR analysis of TOX mRNA level in CD8+ T cells treated with Kyn at indicated concentrations (0, 50, 100, and 200 μM) for 48 h. (F) qRT-PCR analysis of TOX mRNA level in CD8+ T cells treated with Kyn for indicated time points (0, 12, 24, 48 h) at 200 μM. (G) qRT-PCR analysis of TOX mRNA level was performed in CD8+ T cell-Scr, CD8+ T cell-T-siTOX#1, and CD8+ T cell-siTOX #2-bearing mice (n = 6/group). (H, I) Exhaustion marker expressions and cytokine production were detected in CD45.1+CD8+ T-cell-Scr treated with DMSO, CD45.1+CD8+ T-cell-Scr treated with kyn (200 μM), CD45.1+CD8+ T-cell-siTOX#1 treated with kyn (200 μM) and CD45.1+CD8+ T-cell-siTOX#2 treated with kyn (200 μM) (n = 6/group). (J) Chromatin immunoprecipitation analysis of TOX binding to PD-1, CTLA-4, and LAG3 promoters treated with 200 μM kynurenine for 48 h. (K) Dual-luciferase reporter assay of TOX overexpression on PD-1, CTLA-4, and LAG3 promoters in NIH3T3 cells. *P < 0.05, **P < 0.01, n.s no significant difference. (L, M) Exhaustion marker expressions and cytokine production were detected. C57BL/6 mice bearing MC38-OVA were adoptively transferred with CD45.1+OT-1 cells (5×10^5/mouse, every 3 days for 3 times) on three occasions (n = 6). At the same time, mice were treated with either DMSO (Transfer NC) or Kyn (50 mg/mouse, every 3 days) for 9 days. CD45.1+CD8+ T cells were isolated from tumor for flow-cytometric analysis. *P < 0.05, **P < 0.01, n.s no significant difference. All data of this figure was analyzed by 1-way ANOVA. The data represent mean ± SEM.

(**Figure 4E**), indicating that IDO1 activity in the tumor microenvironment facilitated tumor growth in the murine CRC model. To confirm the potential role of IDO1 inhibitors in CRC treatment, MC38- and CT26-bearing mice were established and treated with different pharmaceuticals strategies. As expected, the therapeutic effect against CRC was generated by the IDO1 inhibitor 1-MT or NLG919 alone and enhanced by anti-PD-1 blockade therapy (**Figure 4F-J**). Consistently, using both 1MT and NLG919, *in vivo* treatment remarkably and effectively activated CD8+ TIL responses, characterized by PD-1, CTLA-4, and LAG3 downregulation and increased IFN-γ and TNF-α production (**Figure 4K-N**). Collectively, our *in vivo* experiments suggested that the exhaustion of CD8+ TILs in patients with CRC was regulated through tumor cell-derived IDO1 activity.

Discussion

ICI immunotherapies using PD-1 blocking antibody have emerged as a standard treatment for metastatic CRC. However, many patients, particularly those with dMMR-MSI-H CRC, poorly respond to ICI immunotherapies [31, 32]. In the present study, we identified IDO1/Kyn activity in tumor microenvironment as an important regulator of CD8+ T-cell exhaustion by upregulating TOX expression in patients with CRC. Our study also demonstrated that the combined blockade of IDO1 activity and PD-1 effectively improved therapeutic efficacy and restored CD8+ T cell-mediated antitumor immune responses in the murine CRC tumor model.

Altered metabolism has been demonstrated to be critical for unconstrained tumor cell proliferation, and tryptophan is considered fundamental for tumor progression [33-37]. IDO1 catabolized the conversion of tryptophan into Kyn, and targeting the IDO1 pathway has produced encouraging results in various cancer types [38]. IDO1 can be expressed by both tumor and myeloid cells. A previous study found higher IDO1 expression during tumor invasion, with IDO1 being suggested as an independent prognostic indicator of CRC [39]. Taker et al. used $IDO1^{-/-}$ mice and observed reduced colitis-associated tumorigenesis in $IDO1^{-/-}$ mice [40]. Consistent with their findings, we found that IDO1 might be a prognostic marker for CRC because IDO1 expression was found to be higher in the late stage than in the early stage of CRC.

1-MT or NLG919 alone could significantly inhibit tumorigenesis and enhance survival rate in MC38- and CT26-bearing mice. The high IDO1 activity in tumor microenvironment has been confirmed to promote CRC progression. In advanced non-small-cell lung cancer, a higher Kyn/trp ratio can predict resistance to anti-PD-1 treatment [41]. Moreover, patients with recurrent glioblastoma who failed to respond to anti-PD-1 treatment demonstrated a strong survival benefit from IDO inhibitor therapy, anti-PD-1 mAb therapy, and triple-agent radiotherapy [42]. Because IDO1 inhibitor combined with PD-1 ICI in CRC treatment has been found to remarkably improve the therapeutic outcome in a murine CRC tumor model, our investigations also provided future perspectives in targeting

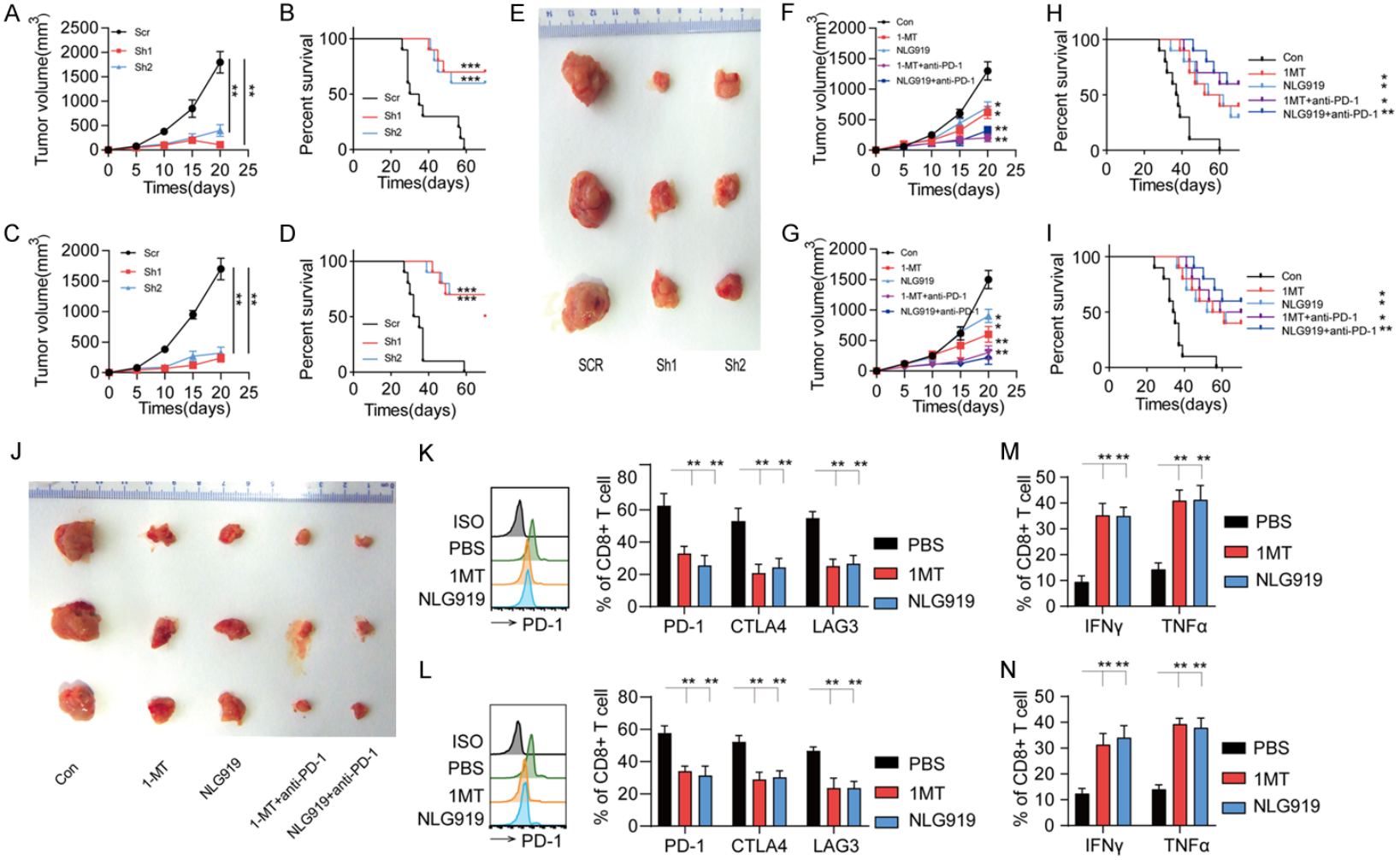

Figure 4. IDO1 blockade improves the therapeutic outcome of CRC by reversing CD8+ T-cell exhaustion status. At a density of 5 × 10^5, MC38-Scr, MC38-IDO1-sh1, and MC38-IDO1-sh2 or CT26-Scr, CT26-IDO1-sh1, and CT26-IDO1-sh2 cells were subcutaneously inoculated into 8-week-old female C57BL/6J and BALB/C mice. (A, C) Tumor dimensions were measured using an electronic caliper every 5 days. Overall tumor volumes were calculated as follows: shortest diameter^2 × longest diameter/2. (B, D) The overall survival of each mice is presented through Kaplan-Meier survival curves. (E) Effects of IDO1 knockdown on the size of CT26 tumors in BALB/C mice. C57BL/6 or BALB/C mice were inoculated with MC38 or CT26 cells. Intraperitoneal injection with DMSO, 1-MT (50 μg), and NLG919 (50 μg) 5 days after the tumor cell inoculation (n = 6/group, every 2 days, 5 times) combined with anti-PD-1 (100 μg, every 2 days, twice). (F, G) Tumor dimensions were measured using an electronic caliper every 5 days. Overall tumor volumes were calculated as follows: shortest diameter^2 × longest diameter/2. (H, I) The overall survival of each mice is presented through Kaplan-Meier survival curves. (J) Effects of different treatment on the size of CT26 tumors in BALB/C mice. (K-M) Flow cytometry

analysis of PD-1, CTLA-4, and LAG3 expressions as well as cytokine production in CD8+ TIL cells isolated from MC38 tumor tissue (n = 6/group). (L-N) Flow cytometry analysis of PD-1, CTLA-4, and LAG3 expressions as well as cytokine production in CD8+ TIL cells isolated from CT26 tumor tissue (n = 6/group). *P < 0.05, **P < 0.01, n.s no significant difference. (A, C, F and G) were analyzed by Student's t test. (B, D, H and I) were analyzed by Log Rank test. (K-N) were analyzed by 1-way ANOVA. The data represent mean ± SEM (A-D, F-I, K-N).

both IDO1/Kyn and PD-1 pathways for the clinical treatment of CRC.

The significant finding in this study is that we first demonstrated that the IDO/Kyn pathway in the CRC tumor microenvironment induced CD8+ TIL exhaustion. Further mechanistic study revealed that the IDO/Kyn pathway induced CD8+ T-cell exhaustion by regulating TOX activity. TOX was recently identified as a central regulator of exhausted T cells in mice, and exhausted T cells cannot be formed in the absence of TOX [43-45]. Kim et al. observed that tumor cells produced vascular endothelial growth factor-A (VEGF-A), which could induce CD8+ T-cell exhaustion in a TOX concentration-dependent manner in CRC. They also demonstrated that combined blockade of PD-1 and VEGF-A resulted in better tumor control by restoring T cell-mediated antitumor function [46]. Consistent with previous encouraging findings, we proposed that the therapeutic outcome of ICI therapy in CRC can be enhanced by anti-PD-1 mAb therapy. VEGF-A and IDO1/Kyn triple blockade might be a promising clinical treatment for CRC, particularly for patients with dMMR-MSI-H CRC who poorly respond to ICI therapies.

Conclusion

In conclusion, we found the role of the IDO1/Kyn pathway in shaping CD8+ TIL-mediated immune responses in CRC. We elucidated that tumor cell-derived IDO1/Kyn promotes CD8+ T-cell exhaustion by regulating TOX activity. Our findings provide a potential implication for combining the IDO1/Kyn and PD-1/PD-L1 pathways in immunotherapy for patients with anti-PD-1-resistant CRC.

Acknowledgements

This work is supported by Liaoning Natural & Science Foundation for Dandan Wu (No. 2019-ZD-0813) and Liaoning Education Foundation for Yufeng Zhu (No. JYTJCZR201904).

Disclosure of conflict of interest

None.

Address correspondence to: Dr. Yufeng Zhu, Department of General Surgery, The First Affiliated Hospital of Jinzhou Medical University, No. 2, Section 5, Renmin Road, Jinzhou 121000, China. E-mail: daniel850205@126.com

References

[1] Hashimoto M, Kamphorst AO, Im SJ, Kissick HT, Pillai RN, Ramalingam SS, Araki K and Ahmed R. CD8 T cell exhaustion in chronic infection and cancer: opportunities for interventions. Annu Rev Med 2018; 69: 301-318.

[2] McLane LM, Abdel-Hakeem MS and Wherry EJ. CD8 T cell exhaustion during chronic viral infection and cancer. Annu Rev Immunol 2019; 37: 457-495.

[3] Wherry EJ. T cell exhaustion. Nat Immunol 2011; 12: 492-499.

[4] Wherry EJ and Kurachi M. Molecular and cellular insights into T cell exhaustion. Nat Rev Immunol 2015; 15: 486-499.

[5] Sharma P and Allison JP. The future of immune checkpoint therapy. Science 2015; 348: 56-61.

[6] Guo X, Zhang Y, Zheng L, Zheng C, Song J, Zhang Q, Kang B, Liu Z, Jin L, Xing R, Gao R, Zhang L, Dong M, Hu X, Ren X, Kirchhoff D, Roider HG, Yan T and Zhang Z. Global characterization of T cells in non-small-cell lung cancer by single-cell sequencing. Nat Med 2018; 24: 978-985.

[7] Wei SC, Levine JH, Cogdill AP, Zhao Y, Anang NAS, Andrews MC, Sharma P, Wang J, Wargo JA and Pe'er D. Distinct cellular mechanisms underlie anti-CTLA-4 and anti-PD-1 checkpoint blockade. Cell 2017; 170: 1120-1133.

[8] Taggart D, Andreou T, Scott KJ, Williams J, Rippaus N, Brownlie RJ, Ilett EJ, Salmond RJ, Melcher A and Lorger M. Anti-PD-1/anti-CTLA-4 efficacy in melanoma brain metastases depends on extracranial disease and augmentation of CD8+ T cell trafficking. Proc Natl Acad Sci U S A 2018; 115: 1540-1549.

[9] Im SJ, Hashimoto M, Gerner MY, Lee J, Kissick HT, Burger MC, Shan Q, Hale JS, Lee J and Nasti TH. Defining CD8+ T cells that provide the proliferative burst after PD-1 therapy. Nature 2016; 537: 417-421.

[10] Demaria O, Cornen S, Daëron M, Morel Y, Medzhitov R and Vivier E. Harnessing innate immunity in cancer therapy. Nature 2019; 574: 45-56.

[11] Gopalakrishnan V, Spencer CN, Nezi L, Reuben A, Andrews MC, Karpinets TV, Prieto PA, Vicente D, Hoffman K, Wei SC, Cogdill AP, Zhao L, Hudgens CW, Hutchinson DS, Manzo T, Petaccia de Macedo M, Cotechini T, Kumar T, Chen WS, Reddy SM, Szczepaniak Sloane R, Galloway-Pena J, Jiang H, Chen PL, Shpall EJ, Rezvani K, Alousi AM, Chemaly RF, Shelburne S, Vence LM, Okhuysen PC, Jensen VB, Swennes AG, McAllister F, Marcelo Riquelme Sanchez E, Zhang Y, Le Chatelier E, Zitvogel L, Pons N, Austin-Breneman JL, Haydu LE, Burton EM, Gardner JM, Sirmans E, Hu J, Lazar AJ, Tsujikawa T, Diab A, Tawbi H, Glitza IC, Hwu WJ, Patel SP, Woodman SE, Amaria RN, Davies MA, Gershenwald JE, Hwu P, Lee JE, Zhang J, Coussens LM, Cooper ZA, Futreal PA, Daniel CR, Ajami NJ, Petrosino JF, Tetzlaff MT, Sharma P, Allison JP, Jenq RR and Wargo JA. Gut microbiome modulates response to anti-PD-1 immunotherapy in melanoma patients. Science 2018; 359: 97-103.

[12] Havel JJ, Chowell D and Chan TA. The evolving landscape of biomarkers for checkpoint inhibitor immunotherapy. Nat Rev Cancer 2019; 19: 133-150.

[13] Le DT, Durham JN, Smith KN, Wang H, Bartlett BR, Aulakh LK, Lu S, Kemberling H, Wilt C, Luber BS, Wong F, Azad NS, Rucki AA, Laheru D, Donehower R, Zaheer A, Fisher GA, Crocenzi TS, Lee JJ, Greten TF, Duffy AG, Ciombor KK, Eyring AD, Lam BH, Joe A, Kang SP, Holdhoff M, Danilova L, Cope L, Meyer C, Zhou S, Goldberg RM, Armstrong DK, Bever KM, Fader AN, Taube J, Housseau F, Spetzler D, Xiao N, Pardoll DM, Papadopoulos N, Kinzler KW, Eshleman JR, Vogelstein B, Anders RA and Diaz LA Jr. Mismatch repair deficiency predicts response of solid tumors to PD-1 blockade. Science 2017; 357: 409-413.

[14] Rizvi NA, Hellmann MD, Snyder A, Kvistborg P, Makarov V, Havel JJ, Lee W, Yuan J, Wong P, Ho TS, Miller ML, Rekhtman N, Moreira AL, Ibrahim F, Bruggeman C, Gasmi B, Zappasodi R, Maeda Y, Sander C, Garon EB, Merghoub T, Wolchok JD, Schumacher TN and Chan TA. Cancer immunology. Mutational landscape determines sensitivity to PD-1 blockade in non-small cell lung cancer. Science 2015; 348: 124-128.

[15] Routy B, Le Chatelier E, Derosa L, Duong CPM, Alou MT, Daillère R, Fluckiger A, Messaoudene M, Rauber C, Roberti MP, Fidelle M, Flament C, Poirier-Colame V, Opolon P, Klein C, Iribarren K, Mondragón L, Jacquelot N, Qu B, Ferrere G, Clémenson C, Mezquita L, Masip JR, Naltet C, Brosseau S, Kaderbhai C, Richard C, Rizvi H, Levenez F, Galleron N, Quinquis B, Pons N, Ryffel B, Minard-Colin V, Gonin P, Soria JC, Deutsch E, Loriot Y, Ghiringhelli F, Zalcman G, Goldwasser F, Escudier B, Hellmann MD, Eggermont A, Raoult D, Albiges L, Kroemer G and Zitvogel L. Gut microbiome influences efficacy of PD-1-based immunotherapy against epithelial tumors. Science 2018; 359: 91-97.

[16] Ganesh K, Stadler ZK, Cercek A, Mendelsohn RB, Shia J, Segal NH and Diaz LA. Immunotherapy in colorectal cancer: rationale, challenges and potential. Nat Rev Gastroenterol Hepatol 2019; 16: 361-375.

[17] Thrumurthy SG, Thrumurthy SS, Gilbert CE, Ross P and Haji A. Colorectal adenocarcinoma: risks, prevention and diagnosis. BMJ 2016; 354: i3590.

[18] Tilg H, Adolph TE, Gerner RR and Moschen AR. The intestinal microbiota in colorectal cancer. Cancer Cell 2018; 33: 954-964.

[19] Lenz HJ, Van Cutsem E, Limon M, Wong K, Hendlisz A, Aglietta M, Garcia-Alfonso P, Neyns B, Luppi G and Cardin D. LBA18_PR Durable clinical benefit with nivolumab (NIVO) plus low-dose ipilimumab (IPI) as first-line therapy in microsatellite instability-high/mismatch repair deficient (MSI-H/dMMR) metastatic colorectal cancer (mCRC). Ann Oncol 2018; 29: mdy424, 019.

[20] Dudley JC, Lin MT, Le DT and Eshleman JR. Microsatellite instability as a biomarker for PD-1 blockade. Clin Cancer Res 2016; 22: 813-820.

[21] Yaghoubi N, Soltani A, Ghazvini K, Hassanian SM and Hashemy SI. PD-1/PD-L1 blockade as a novel treatment for colorectal cancer. Biomed Pharmacother 2019; 110: 312-318.

[22] Le DT, Uram JN, Wang H, Bartlett BR, Kemberling H, Eyring AD, Skora AD, Luber BS, Azad NS and Laheru D. PD-1 blockade in tumors with mismatch-repair deficiency. N Engl J Med 2015; 372: 2509-2520.

[23] Siska PJ and Rathmell JC. T cell metabolic fitness in antitumor immunity. Trends Immunol 2015; 36: 257-264.

[24] Agus A, Planchais J and Sokol H. Gut microbiota regulation of tryptophan metabolism in health and disease. Cell Host Microbe 2018; 23: 716-724.

[25] Cheong JE and Sun L. Targeting the IDO1/TDO2-KYN-AhR pathway for cancer immunotherapy - challenges and opportunities. Trends Pharmacol Sci 2018; 39: 307-325.

[26] Roager HM and Licht TR. Microbial tryptophan catabolites in health and disease. Nat Commun 2018; 9: 3294.

[27] Savitz J. The kynurenine pathway: a finger in every pie. Mol Psychiatry 2020; 25: 131-147.

[28] Dagenais-Lussier X, Aounallah M, Mehraj V, El-Far M, Tremblay C, Sekaly RP, Routy JP and Van Grevenynghe J. Kynurenine reduces memory CD4 T-cell survival by interfering with interleu-

kin-2 signaling early during HIV-1 infection. J Virol 2016; 90: 7967-7979.
[29] Lim CK, Bilgin A, Lovejoy DB, Tan V, Bustamante S, Taylor BV, Bessede A, Brew BJ and Guillemin GJ. Kynurenine pathway metabolomics predicts and provides mechanistic insight into multiple sclerosis progression. Sci Rep 2017; 7: 41473.
[30] Liu Y, Liang X, Dong W, Fang Y, Lv J, Zhang T, Fiskesund R, Xie J, Liu J and Yin X. Tumor-repopulating cells induce PD-1 expression in CD8+ T cells by transferring kynurenine and AhR activation. Cancer Cell 2018; 33: 480-494.
[31] Overman MJ, McDermott R, Leach JL, Lonardi S, Lenz HJ, Morse MA, Desai J, Hill A, Axelson M and Moss RA. Nivolumab in patients with metastatic DNA mismatch repair-deficient or microsatellite instability-high colorectal cancer (CheckMate 142): an open-label, multicentre, phase 2 study. Lancet Oncol 2017; 18: 1182-1191.
[32] Le DT, Durham JN, Smith KN, Wang H, Bartlett BR, Aulakh LK, Lu S, Kemberling H, Wilt C and Luber BS. Mismatch repair deficiency predicts response of solid tumors to PD-1 blockade. Science 2017; 357: 409-413.
[33] Pilotte L, Larrieu P, Stroobant V, Colau D, Dolušić E, Frédérick R, De Plaen E, Uyttenhove C, Wouters J and Masereel B. Reversal of tumoral immune resistance by inhibition of tryptophan 2, 3-dioxygenase. Proc Natl Acad Sci U S A 2012; 109: 2497-2502.
[34] DeBerardinis RJ and Chandel NS. Fundamentals of cancer metabolism. Sci Adv 2016; 2: e1600200.
[35] Pavlova NN and Thompson CB. The emerging hallmarks of cancer metabolism. Cell Metab 2016; 23: 27-47.
[36] Peiris-Pagès M, Martinez-Outschoorn UE, Pestell RG, Sotgia F and Lisanti MP. Cancer stem cell metabolism. Breast Cancer Res 2016; 18: 55.
[37] Vander Heiden MG and DeBerardinis RJ. Understanding the intersections between metabolism and cancer biology. Cell 2017; 168: 657-669.
[38] Soliman H, Antonia S, Sullivan D, Vanahanian N and Link C. Overcoming tumor antigen anergy in human malignancies using the novel indeolamine 2, 3-dioxygenase (IDO) enzyme inhibitor, 1-methyl-D-tryptophan (1MT). J Clin Oncol 2009; 27: 3004-3004.
[39] Ferdinande L, Decaestecker C, Verset L, Mathieu A, Lopez XM, Negulescu AM, Van Maerken T, Salmon I, Cuvelier C and Demetter P. Clinicopathological significance of indoleamine 2, 3-dioxygenase 1 expression in colorectal cancer. Br J Cancer 2012; 106: 141-147.
[40] Thaker AI, Rao MS, Bishnupuri KS, Kerr TA, Foster L, Marinshaw JM, Newberry RD, Stenson WF and Ciorba MA. IDO1 metabolites activate β-catenin signaling to promote cancer cell proliferation and colon tumorigenesis in mice. Gastroenterology 2013; 145: 416-425.
[41] Botticelli A, Cerbelli B, Lionetto L, Zizzari I, Salati M, Pisano A, Federica M, Simmaco M, Nuti M and Marchetti P. Can IDO activity predict primary resistance to anti-PD-1 treatment in NSCLC. J Transl Med 2018; 16: 1-6.
[42] Ladomersky E, Zhai L, Lenzen A, Lauing KL, Qian J, Scholtens DM, Gritsina G, Sun X, Liu Y and Yu F. IDO1 inhibition synergizes with radiation and PD-1 blockade to durably increase survival against advanced glioblastoma. Clin Cancer Res 2018; 24: 2559-2573.
[43] Khan O, Giles JR, McDonald S, Manne S, Ngiow SF, Patel KP, Werner MT, Huang AC, Alexander KA and Wu JE. TOX transcriptionally and epigenetically programs CD8+ T cell exhaustion. Nature 2019; 571: 211-218.
[44] Seo H, Chen J, González-Avalos E, Samaniego-Castruita D, Das A, Wang YH, López-Moyado IF, Georges RO, Zhang W and Onodera A. TOX and TOX2 transcription factors cooperate with NR4A transcription factors to impose CD8+ T cell exhaustion. Proc Natl Acad Sci U S A 2019; 116: 12410-12415.
[45] Wang X, He Q, Shen H, Xia A, Tian W, Yu W and Sun B. TOX promotes the exhaustion of antitumor CD8+ T cells by preventing PD1 degradation in hepatocellular carcinoma. J Hepatol 2019; 71: 731-741.
[46] Kim CG, Jang M, Kim Y, Leem G, Kim KH, Lee H, Kim TS, Choi SJ, Kim HD and Han JW. VEGF-A drives TOX-dependent T cell exhaustion in anti-PD-1-resistant microsatellite stable colorectal cancers. Sci Immunol 2019; 4: eaay0555

Table S1. Patient information

Patients NO.	Age	Gender	Status
1	56	F	III
2	70	M	II
3	49	F	III
4	81	F	III
3	55	M	I
5	55	M	I
6	63	M	II
7	60	F	I
8	41	M	III
9	49	F	I
10	55	F	III
11	62	M	IV
12	68	F	IV
13	67	F	II
14	42	M	I
15	45	M	III
16	49	M	I
17	70	F	IV
18	51	F	IV
19	59	M	III
20	71	F	II

Abbreviations M: male, F: female.

Table S2. Monoclonal antibodies and fluorochromes used

Antibody	Fluorochrome	Clone	Provider
CD45.1	Alexa Fluor 700	A20	BioLegend
PD-1	FITC	29F.1A12	BioLegend
CTLA4	PE	UC10-4B9	BioLegend
LAG3	PE/Cy7	C9B7W	BioLegend
CD3e	APC	145-2C11	BioLegend
CD8a	Pacific Blue	53-6.7	BioLegend
IFNγ	PE	XMG1.2	BioLegend
TNFα	APC	MAb11	BioLegend
TOX	PE	REA473	Miltenyi Biotec